

Mechanical Properties of Collagen Fibrils on Thin Films by Atomic Force Microscopy Nanoindentation

Kontomaris S.V.*, Stylianou A., Yova D., Politopoulos K.

Biomedical Optics & Applied Biophysics Lab, School ECE, Division of Electromagnetics, Electrooptics & Electronic Materials
National Technical University of Athens
Athens, Greece

*e-mail address: steliosk@central.ntua.gr

Abstract — Atomic Force Microscopy (AFM) is a powerful tool as far as surface characterization is concerned, due to its ability to relate high resolution imaging with mechanical properties. Furthermore biological samples, such as collagen, can be studied by AFM with a non-destructive manner. Collagen is the most abundant protein in mammals and because of its unique properties is widely used as biomaterial. Due to the human skin chronic exposure to sun light and since UV-rays are used in sterilizing and cross linking methods of collagen based biomaterials, the investigation of the influence of UV light on collagen, is crucial. The purpose of this paper was to investigate the topographic features and the mechanical properties of collagen fibrils prior and post ultraviolet (UV) by using the AFM indentation method. Hence, load-displacement curves were obtained on collagen fibrils in order to calculate the Young modulus for each case. Each curve presented, was the average of 10 curves. The results showed that Young modulus value increased after 4 hours of UV irradiation from 0.5 GPa to 1.53 GPa. After 8 hours of UV irradiation the Young modulus value was calculated equal to 3.2 GPa. These experiments yielded a clear stiffening of collagen fibrils as a result of UV exposure. Moreover, after 8 hours of UV exposure, collagen fibrillar structure started to deform and the characteristic D-band of collagen fibrils deteriorated. The investigation of the alterations of the modulus under UV irradiation, will contribute to the clarification of the impact that different physical and chemical parameters have on the mechanical properties of collagen-based materials. In addition, this will enable the design and development of biomaterials with improved properties.

Keywords: AFM, collagen fibrils, nanoindentation, UV.

I. INTRODUCTION

Indentation is a common technique used in testing mechanical properties of materials among which and biological [1-4]. It is based on recording the elastic response of the material by using an indenter. The quantitative parameter for the determination of material elastic properties is stiffness which describes the relation between an applied, nondestructive load and the resultant deformation. It can be determined at all scales of a material structure even in extremely low dimensions by using micro- or nanoindenter, i.e. nanoindentation. Stiffness can be sensitive to the structural and mechanical properties of heterogeneous materials and thus can be used as a probe of hierarchical structure-property relationships [1]. Atomic Force Microscopy (AFM) is

increasingly being used to measure the mechanical properties of the sample with a micro- or nanometric resolution. The use of AFM for nanoindentation research purposes was mainly driven by the need of combining high resolution images with mechanical properties. AFM consists mostly of a cantilever and a very sharp tip. The tip is mounted at the end of the cantilever. The surface of each sample is scanned by the tip, and the whole procedure is recorded by a computer, which is connected to the AFM. The computer then reconstructs the 3D topography of the scanned area of the sample using the minute deflections of the cantilever [5].

AFM stiffness measurements depend on monitoring the cantilever deflection during the movement of the tip toward the sample surface. The curve displaying the force applied as a function of the tip indentation is referred to as a force-indentation (F-I) curve [4]. Indentation curve can be used for acquisition of stiffness in order to determine elastic properties of the sample surface. However, stiffness is not a suitable parameter for the characterization of a material elasticity because its value depends on the deformation geometry. Hence, the material elasticity must be characterized by its Young modulus value. The Young modulus allows the estimation of the force, which is required to generate a certain deformation of the material and it depends only on the material properties [5].

As it is well known, the most common protein in mammals is collagen. Most parts of the mammal body, for example tissue, skin, bone, cartilage, or tendons contain collagen in the form of collagen fibrils. The results of a number of studies with collagen films show that the cell response can be easily determined, if the mechanical properties of the larger collagen fibrils can be defined [6]. Collagen fibrils, depending on the tissue, are aligned laterally to form bundles and fibers, which among other properties offer to the tissue mechanical strength and stability.

In order to define and measure fibrils mechanical properties with AFM, collagen thin films can be used. AFM can be used for characterizing those films surface in nanoscale [7] and offers qualitative and quantitative information [8]. Furthermore, collagen thin films can be used for investigating the influence of different parameters and combining them with other properties like optical ones [9,10].

The purpose of this paper was to investigate mechanical properties of collagen fibrils prior and post ultraviolet (UV) irradiation. The influence of UV rays on collagen is crucial due to human skin chronic exposure to sun light and since UV light is used in sterilizing and cross-linking methods of collagen based materials. In this paper Young's modulus of collagen fibrils on collagen thin films that were irradiated with UV radiation for various time intervals was measured. The investigation of the alterations of collagen Young's modulus, under UV radiation, will contribute to the clarification of the effect of different physical and chemical parameters on the mechanical properties of collagen. This research will contribute in both the design and development of biomaterials with improved properties.

II. METHOD

In practice, the indentation is performed by moving the sample up and down toward the tip and measuring the corresponding deflection of the cantilever in order to create a force-displacement curve [4]. A force-displacement curve is generated at a single location on the sample surface by measuring how much the cantilever bends during one or more up and down movements of the scanner on which the sample is based. The deflection of the cantilever corresponds to the applied force on the sample by using the simple equation $F=kd$ where d is the deflection of the cantilever, k the cantilever spring constant and F is the applied force. The force-displacement curve consists of two parts, the loading curve in which the sample movement is towards the tip and the unloading curve in which the sample movement is the opposite, i.e. away from the tip (Figure 1).

Briefly, the far right side of the curve represents the area in which the scanner tube is fully retracted. This is also the starting point before a curve is taken. The net force on the cantilever at this point should be zero (the cantilever is undeflected). As the scanner tube is extended (moving to the left in Figure 1), the tip jumps onto the sample due to the attractive (negative) interatomic force (snap in point in Figure 1). At this point the cantilever bends toward the surface (negative net force).

The scanner continues to extend, until the cantilever is bent away from the surface. The net force on the cantilever is positive (repulsive). After the scanner tube is fully extended, it begins to retract (moving to the right in Figure 1). The force on the cantilever follows a different path. The horizontal offset between the initial and the return paths takes place due to scanner hysteresis. This deflection of the cantilever is shown in Figure 1 as region b, where the net force on the cantilever is strongly negative.

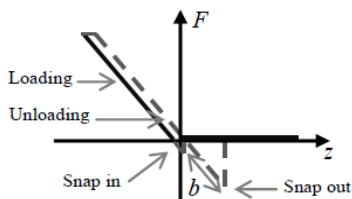


Figure 1. Typical loading-unloading curves in case of a hard sample exposed in air.

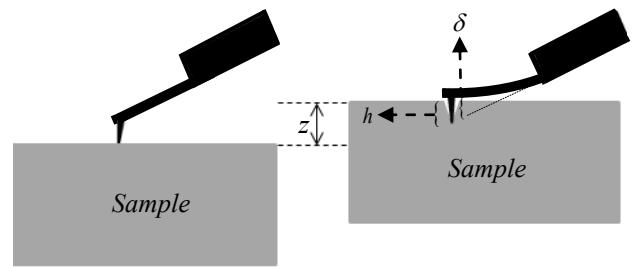


Figure 2. Sample moves toward the tip. The piezomovement of the sample z is equal to deflection of the cantilever δ plus the indentation depth h .

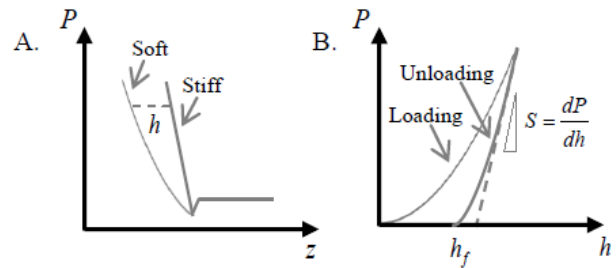


Figure 3. A) Retracting load-displacement curves of soft and stiff sample: Vertical axis (P) represents the applied load and the horizontal axis (z) the motion of the sample. The region in the right side of the diagram is the non-touching region, where the sample surface is away from the tip. B) Schematic illustration of load-indentation curves. The vertical axis represents the applied load (P) and the horizontal (h) the indentation depth.

In case of soft biological samples, the motion towards the tip is larger than the deflection of the cantilever and therefore the applied force is overestimated. Thus the cantilever deflection, δ (the displacement of the AFM tip), is smaller than the piezo-movement of the sample z , so the relation between these displacements is $z=\delta+h$ where h is the indentation depth (Figure 2). Hence, the difference between the sample motion and the cantilever deflection is the deformation of the sample surface, i.e. the indentation depth.

Thus for an AFM indentation procedure, a reference sample must be first used. This sample must be several orders of magnitude stiffer than the AFM tip, in order not to be intended. In this case the piezomovement of the sample is equal to the cantilever deflection since no indentation occurs. The force-displacement curve for a stiff sample is linear, since the indenter force is proportional to the cantilever deflection. The next step is the acquisition of the force-displacement curve for the soft sample of interest (Figure 3A).

Load - indentation curve, is used for determining the material contact stiffness [4,11,12] (Figure 3B). As it has already been mentioned, the load - indentation curve results from the difference in the displacement of a stiff and a soft sample so as to succeed the same deflection of the cantilever (i.e. the same applied load).

According to the Oliver-Pharr method [4] (which leads to Young's modulus calculation), the contact stiffness can be obtained from the unloading part of the load-indentation curve which is considered to fit in the following equation:

$$p = B(h - h_f)^m \quad (1)$$

where p is the indenter load (i.e. the indenter force), h is the vertical displacement of the indenter, h_f is the final unloading depth, and B , m are fitting factors.

Stiffness is given by the slope of the upper unloading part of the curve, as follows:

$$S = \frac{dp}{dh} \quad (2)$$

The stiffness value leads to the estimation of the Young's modulus, under the condition that the shape of the tip and the Poisson's ratio of the sample are known. The formula that contains both the stiffness and the reduced modulus is:

$$E_r = \frac{\sqrt{\pi}}{2} \cdot \frac{S}{\sqrt{A}} \quad (3)$$

where, E_r is the reduced modulus, ν the Poisson's ratio, S the contact stiffness, and A an area function related to the effective cross-sectional or projecting area of the indenter.

The reduced modulus E_r is the combined elastic modulus of the contacting bodies. The equation that combines the two is given by:

$$\frac{1}{E_r} = \frac{1-\nu^2}{E} + \frac{1-\nu_i^2}{E_i} \quad (4)$$

where, E_i and ν_i , and E and ν , describe the elastic modulus and Poisson ratio of the indenter and the specimen, respectively.

The reduced elastic modulus takes into account the fact that elastic displacements occur in both the specimen, and the indenter. Providing that the tip is several orders of magnitude stiffer than the sample, the second term of the equation above is close to zero, so reduced modulus is formed as follows:

$$\frac{1}{E_r} = \frac{1-\nu^2}{E} \quad (5)$$

In practice, the indenter is usually made of a material much stiffer than the sample. Thus the formula between elastic modulus and stiffness can be written in the following form:

$$E = \frac{\sqrt{\pi}}{2} (1-\nu^2) \frac{S}{\sqrt{A}} \quad (6)$$

This equation gives a very general relation that can be applied to any axisymmetric indenter. It is not limited to a specific simple geometry, even though it is often associated with flat punch indentation [4, 5, 12]. Although it was originally derived for elastic contact only, it has subsequently been shown that it can be applied equally well to elastic-plastic contact. Regarding small indentation depths (Figure 4), pyramidal indenters can be analyzed in terms of a paraboloid of revolution [4].

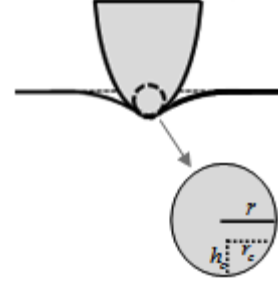


Figure 4. Assumption of a hard pyramidal AFM tip as a paraboloid of revolution. In the case of small indentation depths it can be approximated by a sphere.

The depth at which contact is made between the indenter and the sample during indentation is defined as contact depth h_c .

$$h_c = h_{\max} - \varepsilon \frac{P_{\max}}{S} \quad (7)$$

where, h_{\max} is the maximum indentation depth and ε is a constant that depends on the indenter's geometry. In case of a paraboloid of revolution geometry, the constant is equal to $\varepsilon=0.75$ [4].

In addition, for a paraboloid of revolution, which can be approximated by a sphere for small indentation depths, the contact radius is determined by the following equation [3,4]:

$$r_c = \sqrt{h_c(2r - h_c)} \quad (8)$$

where r is the tip radius and h_c is the contact depth. Thus, the projected area can be derived by the following equation:

$$A_c = \pi r_c^2 \quad (9)$$

where, A_c is the projected area of the tip-sample contact surface [3,12].

It must be noted that during an indentation procedure, the following factors must be considered [4, 11, 12]:

1. The resulted deformation has not only elastic but also a plastic contribution as well.
2. The indentation load must be applied to a semi-infinite half space.
3. The sample is considered to be homogeneous and isotropic in order the Young modulus to be independent from the resulted strain.

III. MATERIALS

A. AFM and Indenter Tips

AFM experiments were carried out using a commercial microscope (CP II, Veeco) in contact mode. For both imaging and indentation tests, pyramidal tips were employed. These tips have a nominal tip radius approximately (\sim) 20 nm on V-shaped cantilevers and a nominal spring constant of 0.5 N/m (type MLCT; Veeco). In order to avoid any damage of the sample during the imaging, a low value of the cantilever

spring constant was chosen. All experiments were performed in air, at room temperature.

The image processing was made by using the image analysis software that accompanied the AFM system DI SPMLab NT ver.60.2 and IP-Image Processing and Data Analysis ver.2.1.15 (Veeco).

B. Collagen Stock Solution

Type I collagen from bovine Achilles tendon (Fluka 27662) was dissolved in acetic acid (CH₃COOH 0.5M) in a final concentration of 8 mg/ml and stored in 4 °C for 24h. The solution was then homogenized at 24000 rpm (Homogenizer IKA T18 Basic) and stored in 4 °C as the stock solution.

C. Collagen Thin Film Formation

The collagen thin films were formed with spin coating (WS-400B-6NPP/LITE Laurell Technologies spin coater). Part of the collagen solution (50 µl) was flushed on the substrate, fresh cleaved mica discs (V1, 9.5 diam., 71856-01 Electron Microscopy Science) and spin coated for 40 sec at 6000 rpm. The procedure was repeated five times so as to form films with multiple collagen layers and in order to avoid measuring mechanical properties of the substrate.

D. Samples Ultraviolet Irradiation

Collagen films, were irradiated under air using a GL4 germicidal lamp with a maximum at 254 nm (Sankyo Denki Co. Ltd., Japan) and a distance of 3cm from the light source for various time intervals was used. The intensity of radiation for this distance was 1813 µW/cm² i.e. 0.11 J/(cm².min) and the dose of incident radiation during the 1 h exposure was 6.6 J/cm². The intensity of the incident light was measured using a Goldilux™ radiometer-photometer (Model 70234-meter and 70239-probe, Oriel Instruments). All measurements were performed in the same conditions of temperature to avoid any influence on the physicochemical and mechanical properties of collagen.

IV. RESULTS

The films that were formed with spin coating method consisted of random oriented collagen fibrils (Figure 5). Moreover, some collagen fibrils present kinks (areas where collagen fibrils change abruptly direction), which it is believed to be mechanical deformations of the fibrils under the influence of the centrifugal forces during the spin coating process. The diameters of collagen fibrils vary from 100nm up to 200nm, while the characteristic D-band were clearly observed (Figure 6). The D-periodicity is a unique characteristic of the formation of collagen fibrils with natural characteristics. Furthermore, it has been reported that D-band plays a significant role in fibrils mechanical strength [13].

The collagen film has been examined, with different levels of UV exposure each time. The first measurement has been obtained without any UV exposure (Figure 7a,b), the second after 4h of UV exposure (Figure 7c,d), and the third after 8h of UV exposure (Figure 7e,f). As far as AFM images are concerned, it is obvious that UV exposure yielded a

deterioration of collagen fibrils. It is evident that after 8h of UV exposure, D-band periodicity does no longer exist. On the contrary the UV-radiation had no effect on the collagen fibril diameters.

Moreover the load – displacement curves of the sample have been obtained each time so as to perform the indentation procedure.

In order to consider that the indentation load is applied to a semiinfinite, elastic-plastic half-space, the tip apex is placed at the center of the collagen fibril during the indentation experiments [11]. The tip apex radius is about 20nm, and this specific value proves that the assumption mentioned above is reasonable due to the fact that the values of the collagen diameters are 5 to 10 times bigger than the tip apex radius.

In order to calculate the stiffness of the collagen fibrils, load–displacement curves were obtained for the collagen film prior UV exposure and post UV exposure (Figure 8). Moreover the stiffness of an infinitely stiff sample (grating) was also measured and as a result its load displacement curve is presented in Figure 8. In the case of a stiff sample the piezo-displacement of the sample towards the tip, is equal to the cantilever deflection, since no indentation occurs. Therefore the slope of load-displacement curve for the stiff sample must be equal to the spring constant of the cantilever ($k=0.5N/m$).

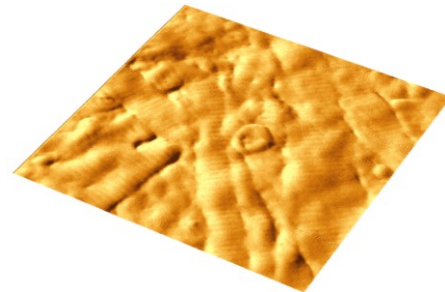


Figure 5. Randomly oriented collagen fibrils.

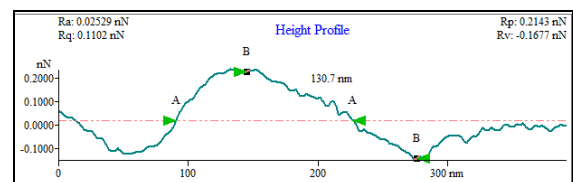
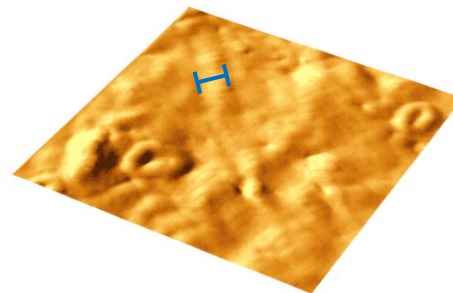


Figure 6. Characteristic collagen fibril before UV irradiation. The diameters of collagen fibrils vary from 100nm up to 200nm.

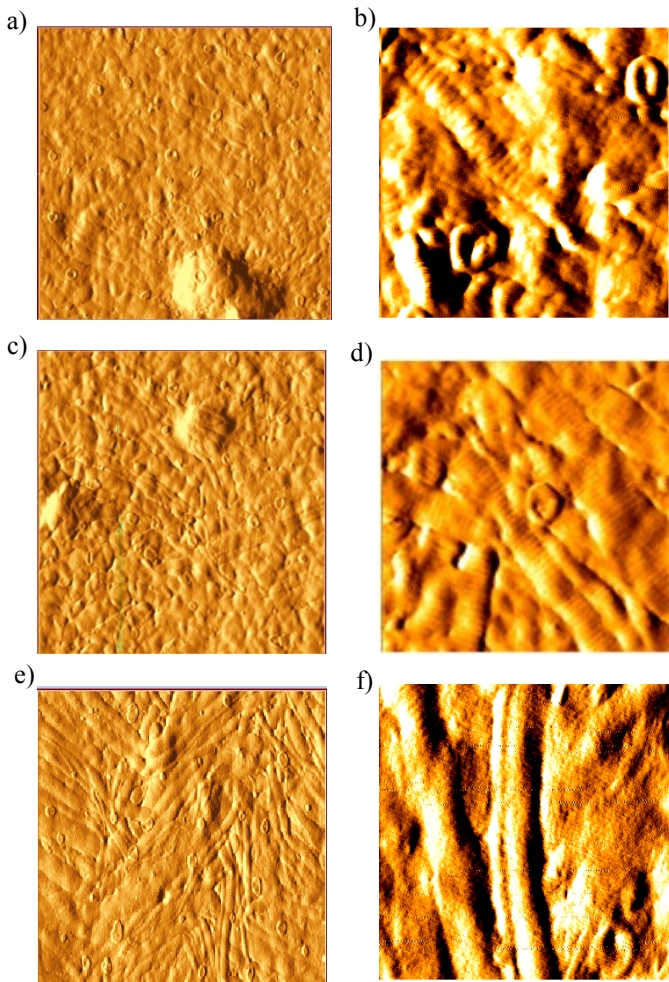


Figure 7. Images of collagen film before and after UV exposure. a, b) $10\mu\text{m} \times 10\mu\text{m}$ and $2\mu\text{m} \times 2\mu\text{m}$ respectively before UV exposure. c, d) $10\mu\text{m} \times 10\mu\text{m}$ and $3\mu\text{m} \times 3\mu\text{m}$ respectively after 4h of UV exposure. e, f) $10\mu\text{m} \times 10\mu\text{m}$ and $3\mu\text{m} \times 3\mu\text{m}$ respectively after 8h of UV exposure.

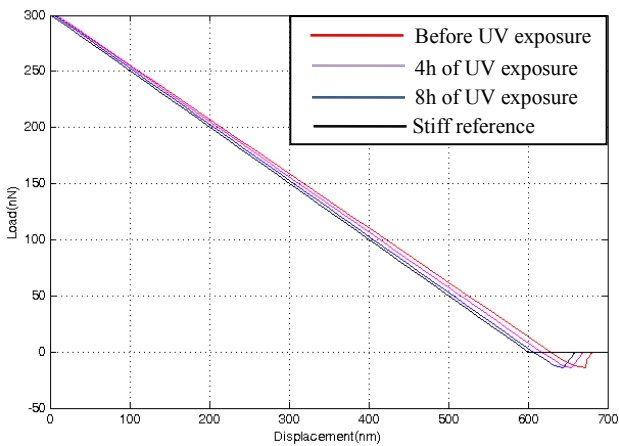


Figure 8. Unloading load-displacement curves obtained by AFM nanoindentation on collagen fibrils, prior UV irradiation (red graph), B) after 4h UV irradiation (magenta graph), after 8h UV irradiation (blue graph). Black graph represents a load-displacement curve obtained on an extremely hard sample (stiff reference).

TABLE I. YOUNG MODULUS VALUES IN RELATION TO IRRADIATION TIME

Time of UV irradiation (h)	Young Modulus (GPa)
0	0.5
4	1.53
8	3.2

The indentation depth in each point can be derived from the displacement difference of a stiff and a soft sample, so as to apply the same load in order to create a load-indentation curve. The load-indentation data are then fitted in equation (1), and the stiffness is calculated by the derivative of the function of the maximum indentation depth. The maximum indentation depth on the sample during the indentation procedure prior UV exposure was 21.1nm. After 4h and 8h of UV exposure, the maximum indentation depth of the sample resulted respectively 9.8nm and 6.1nm. It is obvious that the indentation depths that were obtained in this experiment had very small values. As a result the ideal approximation of the tip is a paraboloid of revolution, since only the tip apex interacts with the sample.

The contact depth which is derived from equation (7), leads to the calculation of contact radius and projected area from equations (8) and (9) respectively.

The Young modulus is estimated from equation (6). For all calculations, the Poisson ratios were assumed to be 0.2. This value is consistent with the literature [6]. However, the exact value of the Poisson ratio is expected to have an insignificant effect on the calculated modulus. Thus the Young modulus value (before UV exposure) was calculated $E=0.5\text{GPa}$ (table I). Moreover, the Young modulus values after 4h and 8h of UV exposure were calculated namely with values $E=1.53\text{GPa}$ and $E=3.2\text{GPa}$ respectively (Table I).

V. DISCUSSION

The influence of UV irradiation on topographical features and mechanical properties of collagen fibrils on collagen thin films was examined by AFM contact mode and indentation methods respectively. The results demonstrated that UV irradiation leads to deterioration of both collagen fibrils structure and D-band periodicity. Moreover, UV irradiation had a significant effect on the elastic properties of collagen fibrils, which was quantified by measuring the Young modulus values, prior and post UV irradiation. The Young modulus value before UV exposure is closed to the values that obtained by A. J.Heim et al. [14]. According to this reference, the reduced modulus values of collagen fibrils vary from 1

GPa to 2 GPa in air. Moreover, the results demonstrated that the sample showed a clear stiffening after the 4h of the UV exposure. However, the rate of stiffening that occurred between the first 4h of UV exposure (0h-4h), was a little bit higher than the stiffening occurred in the last 4h of UV exposure (4h-8h). The sample became stiffer as the time went by, but the stiffening was not proportional to the time of exposure. This result is a consequence of the stiffening of the sample after its exposure in UV radiation.

As it has already illustrated, UV irradiation induces an increase in tensile strength because it leads to physical crosslinking [15]. Hence UV irradiation is used to cause collagen scaffold polymerization in order to create more suitable biomaterials for load bearing applications [15]. In addition, as it has been mentioned by A. Sionkowska et. al., who performed tensile experiments in air – dried collagen films, the increasing duration of UV irradiation leads to an increase in Young’s modulus [16]. Even though the above papers are related to tensile experiments, it is evident that UV irradiation increases collagen stiffness. Therefore, UV irradiation can be used to improve the mechanical properties of collagen-based materials [17,18].

VI. CONCLUSION

In this paper, a quantitative research of the UV effects on the mechanical properties and on the topographical features of collagen films in nanoscale and in air environment was investigated by AFM nanoindentation technique. The AFM nanoindentation is a powerful technique which enables the characterization of the mechanical properties of collagen fibrils in the nanoscale. The mechanical properties of collagen fibrils, prior and post UV exposure were determined. The results showed that UV exposure induced an increase of the Young modulus in collagen fibrils, and in the deterioration of collagen D-band periodicity after 8h of exposure. The clarification of the impact that different physical and chemical parameters have on the mechanical properties of collagen-based materials will enable the design and development of biomaterials with improved properties.

REFERENCES

[1] M. Stolz, R. Raiteri, A. U. Daniels, M. R. VanLandingham, W. Baschong, and U. Aebi, “Dynamic elastic modulus of porcine articular cartilage determined at two different levels of tissue organization by indentation–type atomic force microscopy,” *Biophys. J.*, vol. 86, pp. 3269–3283, May 2004.

[2] M. Stolz, R. Gottardi, R. Raiteri, S. Miot, I. Martin, R. Imer, et al., “Early detection of aging cartilage and osteoarthritis in mice and patient samples using atomic force microscopy,” *Nat. Nanotechnol.*, vol. 4, pp. 186–192, February 2009.

[3] M. Loparic, D. Wirz, A. U. Daniels, R. Raiteri, M. R. Van Landingham, G. Guex, et al., “Micro– and nanomechanical analysis of articular cartilage by indentation–type atomic force microscopy: validation with a gel–microfiber composite,” *Biophys. J.*, vol. 98, pp. 2731–2740, June 2010.

[4] W. C. Oliver, G. M. Pharr, “Measurement of hardness and elastic modulus by instrumented indentation: Advances in understanding, and

refinements to methodology,” *J. Mater. Res.*, vol. 19, pp. 3–20, January 2004.

[5] L. Sirghi, “Atomic Force Microscopy indentation of living cells,” in *Microscopy: Science, Technology, Applications and Education*, vol. 1, A. Méndez and V. J. Díaz, Eds Formatex Microscopy series No 4, 2010, pp. 433–440.

[6] K. H. Chung, K. Bhadriraju, T. A. Spurlin, R. F. Cook, and A. L. Plant, “Nanomechanical properties of thin films of type I collagen fibrils,” *Langmuir*, vol. 26, pp. 3629–3636, March 2010.

[7] A. Stylianou, S. B. Kontomaris, M. Kyriazi, and D. Yova, “Surface characterization of collagen films by atomic force microscopy,” *IFMBE Proc.*, vol. 29, 27 May 2010 through 30 May 2010, pp. 612–615.

[8] A. Stylianou, D. Yova., K. Politopoulos, “Atomic force microscopy quantitative and qualitative nanoscale characterization of collagen thin films,” *Emerg. Technol. Non–Destr. Test. V – Proc. Conf. Emerg. Technol. NDT*, 19 September 2011 through 21 September 2011, pp. 415–420.

[9] A. Stylianou, M. Kyriazi, K. Politopoulos, and D. Yova, “Combined SHG signal information with AFM imaging to assess conformational changes in collagen,” *Final Program Abstr. Book – Int. Conf. Inf. Technol. Appl. Biomed.*, ITAB, 4 November 2009 through 7 November 2009.

[10] A. Stylianou, K. Politopoulos, M. Kyriazi and D. Yova, “Combined information from AFM imaging and SHG signal analysis of collagen thin films,” *Biomed. Signal Proces.*, vol. 6 no 3,7 pp. 307–313, July 2011.

[11] M. P. E. Wenger, L. Bozec, M. A. Horton, and P. Mesquidaz, “Mechanical properties of collagen fibrils,” *Biophys. J.*, vol. 93, pp. 1255–1263, August 2007.

[12] A. C. Fischer-Cripps, “The IBIS Handbook of Nanoindentation,” Forestville NSW 2087 Australia, Fischer-Cripps Laboratories Pty Ltd, 2009.

[13] C. A. Grant, M. A. Phillips, N. H. Thomson, “Dynamic mechanical analysis of collagen fibrils at the nanoscale,” *J. Mech. Behav. Biomed. Mater.*, vol. 5, pp. 165–170, Januray 2012.

[14] A. J. Heim, W. G. Matthews, and T. J. Koob, “Determination of the elastic modulus of native collagen fibrils via radial indentation,” *Appl. Phys. Lett.*, vol. 89, art no. 181902, October 2006.

[15] R. Parenteau-Bareil, R. Gauvin and F. Berthod, “Collagen–based biomaterials for tissue engineering applications,” *Materials*, vol. 3, pp. 1863–1887, March 2010.

[16] A. Sionkowska, M. Wisniewski, J. Skopinska, G. F. Poggi, E. Marsano, C. A. Maxwell, T. J. Wess, “Thermal and mechanical properties of UV irradiated collagen/chitosan thin films,” *Polym. Degrad. Stabil.*, vol 91, pp. 3026–3032, September 2006.

[17] G. Fessel, J. Wernli, Y. Li, C. Gerber and J. G. Snedeker, “Exogenous collagen cross-linking recovers tendon functional integrity in an experimental model of partial tear,” *J. Orthop. Res.*, vol. 30, pp. 973–981, June 2012.

[18] A. Gaspar, L. Moldovan, D. Constantin, A. M. Stanciu, P. M. Sarbu Boeti, and I. C. Efrimescu, “Collagen–based scaffolds for skin tissue engineering,” *J. Med. Life.*, vol. 4, pp. 172–177, May 2011.